

Theoretical model for the magnetoelectric effect in magnetostrictive/piezoelectric composites

Idahosa A. Osaretin and Roberto G. Rojas

ElectroScience Laboratory, Department of Electrical and Computer Engineering, The Ohio State University, Columbus, Ohio 43212, USA

(Received 11 August 2010; published 10 November 2010)

A theoretical model for the longitudinal magnetoelectric effect in laminate composites comprising magnetostrictive and piezoelectric phases is presented. The model characterizes the magnetoelectric media in terms of its permeability, permittivity, and magnetoelectric-susceptibility tensor. A distinct approach to model the media is presented, in which fundamental electromagnetic boundary conditions are applied to all fields existing at the interface between the layers, and in the composite material in general. The application of the boundary condition used here represents a change from previous models where quasistatic approximations are used, including open circuit conditions imposed on the electric displacement field. The model presented here takes into account the imperfect coupling in terms of the existing mechanical forces (stress, strain) that can occur at the interface of such layered composites. An interface coupling parameter is used to model the strain relationship between layers of the composite. Results of the theoretical model are compared to experimental data and show much better results than previously obtained.

DOI: [10.1103/PhysRevB.82.174415](https://doi.org/10.1103/PhysRevB.82.174415)

PACS number(s): 75.85.+t, 75.80.+q, 77.65.-j, 77.84.Lf

I. INTRODUCTION

The magnetoelectric (ME) effect has been researched since 1888 when Rontgen discovered that a moving dielectric became magnetized when placed in an electric field.¹ Polarization of a moving dielectric in an applied magnetic field was proven in 1905 by Wilson.² Such materials, which can be generally described as bianisotropic, are defined by constitutive equations in which the electric and magnetic fields are coupled as described below,³

$$\begin{aligned}\mathbf{D} &= \bar{\epsilon}\mathbf{E} + \bar{\xi}\mathbf{H}, \\ \mathbf{B} &= \bar{\zeta}\mathbf{E} + \bar{\mu}\mathbf{H},\end{aligned}\quad (1)$$

where \mathbf{D} , \mathbf{B} , \mathbf{E} , and \mathbf{H} , respectively, are the electric displacement field, magnetic-flux density, electric field, and magnetic field. $\bar{\epsilon}$ and $\bar{\mu}$, respectively, are the permittivity and permeability tensors. $\bar{\xi}$ and $\bar{\zeta}$ are the bianisotropic coupling tensors.

The ME effect is generally defined as the induced electric polarization of a material in an applied magnetic field or the induced magnetization of the material in an applied electric field.⁴ For ME media, the coupling tensors, ζ , and ξ , in Eq. (1) are replaced by the ME susceptibility term, α , such that $\bar{\alpha} = \bar{\zeta} = \bar{\xi}$. The ME effect was hypothesized as possible in non-moving media by Curie in 1894, based upon symmetry considerations⁵ of single-phase crystals. In 1948, the phenomenon received more interest when Tellegen postulated such media in the realization of his gyrator.⁶ A little more than a decade later, Dzyaloshinskii predicted the ME effect in a single-phase material,⁷ antiferromagnetic chromium oxide, Cr_2O_3 . Experimental confirmation of the ME effect in this media was later shown.⁸⁻¹⁰ However, the small magnitude of the induced polarization and/or magnetization obtained from single-phase ME materials made it ineffective for practical applications.¹¹

Realization of much larger ME effect using composite materials was introduced by van Suchtelen in 1972 using a product property¹² between layered piezoelectric and piezomagnetic materials.¹³ Since then, giant ME voltage coefficients (α'_E) have been realized¹⁴⁻¹⁶ using composite layers. However, use of ME materials for device applications have been slowed partly due to a lack of accurate theoretical models to properly simulate the media. The ME voltage coefficient is a parameter that can be used in characterizing the composite. The ME voltage coefficient is related to the ME susceptibility tensor as $\bar{\alpha}' = \epsilon_0 \bar{\epsilon}_r \bar{\alpha}'_E$, where $\bar{\epsilon}_r$ is the relative permittivity tensor of the medium.

Harshe, in 1991, obtained theoretical models¹⁷ for the longitudinal ME voltage coefficient of multilayer composites composed of lead zirconate titanate (PZT) and ferrite layers. However, there were large deviations between the ME voltage coefficient obtained via theoretical modeling and corresponding experimental values of fabricated structures. The experimental results had similar characteristics to those reported in literature but the theoretical results obtained were several times higher. Reasons for the poor agreement between theoretical and experimental results include poor interface coupling between the layers and the inadequate application of boundary conditions on the electromagnetic fields to obtain the model.¹⁷ Since then, other works¹⁸⁻²¹ have looked into obtaining more accurate theoretical models, including a coupling factor for the mismatch at the composite's bonding interface. This was done using an interface coupling parameter that models the strain transfer relationship between the piezoelectric and magnetostrictive phases. The ME voltage coefficients obtained in these works had similar trends as the experimental data, however, there still remained some deviation in the overall magnitude of the ME voltage coefficients, as theoretical results remained several times higher than experimental values. We believe the difference may result from the application of boundary conditions used to obtain the theoretical model, which involve quasistatic approximations, including open circuit conditions on the pi-

ezoelectric phase.^{17,21} The use of this electromagnetic boundary conditions in previous models results in similar theoretical models and resultant theoretical values that are much higher than experimental values.¹⁷

In this discourse, we use a different approach. We apply fundamental electromagnetic wave boundary conditions³ on the fields within the composite structure. We introduce distinct theoretical models for the longitudinal ME effect in a piezoelectric/magnetostrictive bilayer that better approximates the experimental results. The model is obtained by solving the constitutive equations of each layer for the all fields present, and then applying a field-averaging method,²² along with boundary conditions on the components of the fields at the composite interface, to obtain homogenized material properties. The homogenized layer is characterized in terms of its effective permeability, effective permittivity, and the effective ME susceptibility tensor with constitutive equations of the form shown in Eq. (1).

II. MAGNETOELECTRIC COMPOSITE THEORY

In composites, the magnetoelectric effect can be obtained using piezoelectric and magnetostrictive materials in a layered structure. PZT and barium titanate are examples of piezoelectric materials that have been used as ME composite materials.^{17,21} The constitutive relationship for the piezoelectric phase is

$${}^pS_i = {}^pS_{ij}{}^pT_j + {}^pd_{ki}{}^pE_k, \quad (2a)$$

$${}^pD_k = {}^pd_{ki}{}^pT_i + {}^p\epsilon_{kn}{}^pE_n, \quad (2b)$$

$${}^pB_k = {}^p\mu_{kn}{}^pH_n. \quad (2c)$$

In Eq. (2), S , T , E , D , H , and B are, respectively, the strain, stress, electric field, electric displacement field, magnetic field, and the magnetic-flux density. Also, s , d , ϵ , and μ are, respectively, the compliance, piezoelectric, permittivity, and permeability coefficients. The superscript p represents the piezoelectric phase. We include a relationship for the permeability of the piezoelectric phase in its constitutive relationship as observed in Eq. (2c). In order to properly model the media in terms of the fields, all field relationships for each composite phase must be obtained. Hence, one must consider the magnetic-flux/magnetic field relationship of the piezoelectric layer to obtain a homogeneous layer that combines properties of both layers.

Nickel ferrite NiFe_2O_4 and copper ferrite CoFe_2O_4 (CFO) are examples of magnetostrictive materials that have been used in ME composites.^{17,21} Magnetostrictive materials are represented by the constitutive equations

$${}^mS_i = {}^mS_{ij}{}^mT_j + {}^mq_{ki}{}^mH_k, \quad (3a)$$

$${}^mB_k = {}^mq_{ki}{}^mT_i + {}^m\mu_{kn}{}^mH_n, \quad (3b)$$

$${}^mD_k = {}^m\epsilon_{kn}{}^mE_n. \quad (3c)$$

In Eq. (3), q is the piezomagnetic coefficient and superscript m represents the magnetostrictive phase. Here, we have ac-

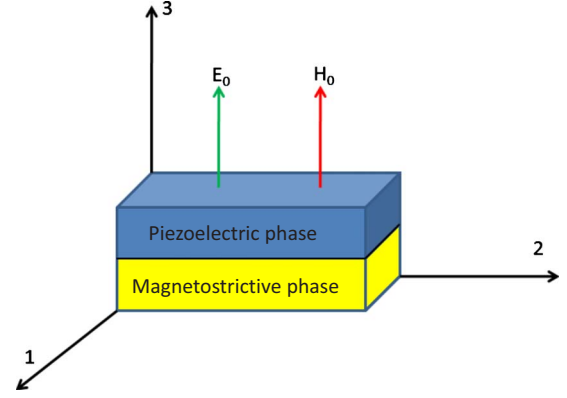


FIG. 1. (Color online) Magnetoelectric composite system diagram. Showing the composite layers and the directions of the poling electric field and the biasing magnetic field for the longitudinal ME effect.

counted for the permittivity of the magnetostrictive phase as can be observed in Eq. (3c), relating the electric field and the electric displacement field.

In our derivation, we only consider the longitudinal ME configuration, in which the composite is poled and biased perpendicular to the interface of the composite as shown in Fig. 1. Although, higher ME voltage coefficients have theoretically been obtained for transverse and in-plane orientations,²¹ we have chosen to model the longitudinal ME configuration because there are experimental results for this orientation in literature.¹⁷ Harshe obtained experimental data for fabricated composites in the longitudinal configuration, hence the published measured results serve as a point of reference.

In modeling the material, we assume that in addition to poling and bias fields within the composite medium, there exist low-frequency fields in all directions which may be time varying. As an example, the fields in the axial direction can be expressed in terms of dc and ac components as

$$\bar{H}_3 = \hat{z}H_0 + \hat{z}H_{ac},$$

$$\bar{E}_3 = \hat{z}E_0 + \hat{z}E_{ac}. \quad (4)$$

The total fields in each respective phase will be represented by a vector field of the form

$${}^{m,p}\mathbf{E} = E_1\hat{1} + E_2\hat{2} + E_3\hat{3},$$

$${}^{m,p}\mathbf{H} = H_1\hat{1} + H_2\hat{2} + H_3\hat{3}. \quad (5)$$

The magnetoelectric effect in composites is a known as a product property^{17,23} due to the resultant interaction between the piezoelectric and magnetostrictive phases to obtain the ME phenomenon. Modeling the ME effect requires an understanding of the strain and stress transfer relationship between the layers of the structure. Bichurin *et al.*²¹ introduced the use of coupling parameter, k , to model the mechanical interaction at the interface between the bilayers. The coupling parameter is defined as $k = ({}^pS_i - {}^pS_{i0}) / ({}^mS_i - {}^pS_{i0})$, ($i=1, 2$), where ${}^pS_{i0}$ is the strain tensor components with no friction

TABLE I. Nonzero coefficients of bulk piezoelectric and magnetostrictive phases.

| Piezoelectric phase | |
|------------------------|--|
| Coefficient type | Nonzero components |
| Permittivity | ${}^p\varepsilon_{11} = {}^p\varepsilon_{22}, {}^p\varepsilon_{33}$ |
| Permeability | ${}^p\mu_{11} = {}^p\mu_{22} = {}^p\mu_{33}$ |
| Compliance | ${}^p s_{11} = {}^p s_{22}, {}^p s_{12} = {}^p s_{21}, {}^p s_{13} = {}^p s_{23} = {}^p s_{31} = {}^p s_{32}, {}^p s_{33},$ ${}^p s_{44} = {}^p s_{55}, {}^p s_{66} = 2({}^p s_{11} + {}^p s_{12})$ |
| Piezoelectric | ${}^p d_{15} = {}^p d_{24}, {}^p d_{31} = {}^p d_{32}, {}^p d_{33}$ |
| Magnetostrictive phase | |
| Permittivity | ${}^m\varepsilon_{11}, {}^m\varepsilon_{22}, {}^m\varepsilon_{33}$ |
| Permeability | ${}^m\mu_{11}, {}^m\mu_{22}, {}^m\mu_{33}$ |
| Compliance | ${}^m s_{11} = {}^m s_{22} = {}^m s_{33}, {}^m s_{44} = {}^m s_{55} = {}^m s_{66}, {}^m s_{12} = {}^m s_{21}$ $= {}^m s_{13} = {}^m s_{23} = {}^m s_{31} = {}^m s_{32}$ |
| Piezoelectric | ${}^m q_{15} = {}^m q_{24}, {}^m q_{31} = {}^m q_{32}, {}^m q_{33}$ |

between phases.²¹ Here, we use a similar coupling parameter, k , as a damping factor to model the strain transfer relationship between the layers. We assume that the strain induced in one phase may not be completely transferred to the adjoining phase due to several factors, which may include mechanical defects and losses, bonding methods, etc. These factors are contained and described by the interface coupling parameter.

In this derivation, as has been previously done, only symmetric or extensional deformation is considered. Such that flexural deformations of the layers that can lead to position-dependent elastic constants are ignored.^{17,21} We make the following assumptions:¹⁸ (i) shear stresses and strains are equal to zero, such that ${}^{m,p}T_i = 0, {}^{m,p}S_i = 0$, for $i = 4, 5$, and 6 . (ii) The thickness of each phase is much smaller than the width and length of the phase. Hence the stress in the axial direction is approximated as zero ${}^m T_3 = {}^p T_3 = 0$. (iii) The strain transfer between phases is related by an interface coupling parameter, k , such that ${}^p S_i = k \cdot {}^m S_i$. (iv) The summation of forces on the in-plane (1-2 plane) boundaries are zero, such that ${}^m T_i^m \nu + {}^p T_i^p \nu = 0$, for $i = 1, 2$, where ${}^m \nu$ and ${}^p \nu$ are the magnetostrictive and piezoelectric volume fractions, respectively, and are defined as ${}^m \nu = \text{volume}^m / \text{volume}^{total}$ and ${}^p \nu = \text{volume}^p / \text{volume}^{total}$.

Solving the constitutive equations of each phase based upon the given assumptions, we obtain the electric displacement field in the piezoelectric region using the nonzero components of the permittivity, permeability, compliance, and piezoelectric coefficient components as shown in Table I. The electric displacement field in the piezoelectric region is derived as

$$\begin{aligned} {}^p D_1 &= {}^p \varepsilon_{11} {}^p E_1, \\ {}^p D_2 &= {}^p \varepsilon_{22} {}^p E_2, \\ {}^p D_3 &= K_1 {}^m H_3 + K_2 {}^p E_3, \end{aligned} \quad (6)$$

where,

$$\begin{aligned} K_1 &= 2{}^p d_{31} {}^m q_{31} k / [k({}^m s_{11} + {}^m s_{12})({}^p \nu / {}^m \nu) + ({}^p s_{11} + {}^p s_{12})], \\ K_2 &= \{-2({}^p d_{31})^2 / [k({}^m s_{11} + {}^m s_{12})({}^p \nu / {}^m \nu) + ({}^p s_{11} + {}^p s_{12})]\} \\ &\quad + {}^p \varepsilon_{33}. \end{aligned} \quad (7)$$

The magnetic-flux density in the piezoelectric region is also required for the theoretical model. It has been described and is easily obtained using Eq. (2c). The form of the permeability tensor can be obtained using the components of the permeability (piezoelectric phase) shown in Table I.

While deriving the magnetic-flux density in the magnetostrictive region, we take into consideration the effect the dc magnetic field bias will have on the ferrite medium. The ME effect in composites is a nonlinear effect. A dc magnetic field bias is usually applied so that the ME effect over a short range around the bias can be approximated as a linear effect.¹⁷ The applied bias, however, has a secondary effect when the magnetostrictive phase is a ferrite material. Ferrites have an intrinsic magnetic moment and application of a dc magnetic field bias will lead to tensor permeability.²⁴ This implies a change to the nonzero permittivity values of the bulk magnetostrictive phase from what had been described in Table I. For the case with the dc magnetic field bias in the axial direction as shown in Fig. 1, the permeability tensor will be of the form²⁴⁻²⁶

$${}^m \mu = \begin{bmatrix} {}^m \mu_{11}^* & {}^m \mu_{12}^* & 0 \\ {}^m \mu_{21}^* & {}^m \mu_{22}^* & 0 \\ 0 & 0 & {}^m \mu_{33}^* \end{bmatrix}. \quad (8)$$

The values of the nonzero components of the permeability as shown in Eq. (8) depends on the intrinsic property of the magnetostrictive phase, such as its magnetization saturation, M_s , and the magnitude of the applied dc magnetic field bias.^{24,25} This change in permeability is a secondary effect from the dc magnetic field bias in the composite structure.¹⁶ This secondary effect obtained in the ferrite material (magnetostrictive phase) is well known and has been used in several device applications based upon the shape and values of the permeability tensor. We do not show here the formulas for the components of the permeability tensor in Eq. (8), as it is readily available in other literature.²⁴⁻²⁶

Solving the magnetostrictive constitutive equations, the magnetic-flux density in the magnetostrictive phase is derived as

$$\begin{aligned} {}^m B_1 &= {}^m \mu_{11}^* {}^m H_1 + {}^m \mu_{12}^* {}^m H_2, \\ {}^m B_2 &= {}^m \mu_{21}^* {}^m H_1 + {}^m \mu_{22}^* {}^m H_2, \\ {}^m B_3 &= C_1 {}^p E_3 + C_2 {}^m H_3, \end{aligned} \quad (9)$$

where,

$$\begin{aligned} C_1 &= 2{}^p d_{31} {}^m q_{31} / [k({}^m s_{11} + {}^m s_{12}) + ({}^p s_{11} + {}^p s_{12})({}^m \nu / {}^p \nu)], \\ C_2 &= \{-2k({}^p q_{31})^2 / [k({}^m s_{11} + {}^m s_{12}) + ({}^p s_{11} + {}^p s_{12})({}^m \nu / {}^p \nu)]\} \\ &\quad + {}^m \mu_{33}^*. \end{aligned} \quad (10)$$

The electric displacement field for the magnetostrictive

phase is required for the theoretical model, and is easily obtained using Eq. (3c) and the nonzero components of the permittivity (magnetostrictive phase) shown in Table I.

III. APPLICATION OF BOUNDARY CONDITIONS

From Maxwell's equations, we deduce conditions involving the normal and tangential fields at the interface. The boundary conditions at the interface, assuming there are no applied surface currents, are³ (i) tangential components of the electric and magnetic fields are continuous across the interface. (ii) Normal components of the electric displacement field and the magnetic-flux density are continuous at the interface. From the first boundary condition, tangential components of the electric and magnetic fields are continuous at the boundary. Thus at the interface,

$$\begin{aligned}\bar{E}_x &= {}^m E_1 = {}^p E_1, \\ \bar{E}_y &= {}^m E_2 = {}^p E_2,\end{aligned}\quad (11a)$$

$$\begin{aligned}\bar{H}_x &= {}^m H_1 = {}^p H_1, \\ \bar{H}_y &= {}^m H_2 = {}^p H_2.\end{aligned}\quad (11b)$$

Here, \bar{E}_x , \bar{E}_y , \bar{H}_x , and \bar{H}_y are the homogenized tangential components of the electric and magnetic field in the ME layer. For ease of understanding, we have chosen to represent all homogenized fields using the (x, y, z) coordinate system than with the $(1\ 2\ 3)$ system used thus far.

We assume the homogenized layer is electrically thin with no field variation across the total thickness of the film. Using a field-averaging method,²² we can define the tangential components of the electric field displacement and the magnetic-flux density as

$$\begin{aligned}\bar{D}_x &= {}^m D_1 {}^m v + {}^p D_1 {}^p v = [{}^m \epsilon_{11} {}^m v + {}^p \epsilon_{11} {}^p v] \bar{E}_x, \\ \bar{D}_y &= {}^m D_2 {}^m v + {}^p D_2 {}^p v = [{}^m \epsilon_{22} {}^m v + {}^p \epsilon_{22} {}^p v] \bar{E}_y,\end{aligned}\quad (12a)$$

$$\bar{B}_x = {}^m B_1 {}^m v + {}^p B_1 {}^p v = [{}^m \mu_{11}^* {}^m v + {}^p \mu_{11} {}^p v] \bar{H}_x + [{}^m \mu_{12}^* {}^m v] \bar{H}_y,$$

$$B_y = {}^m B_2 {}^m v + {}^p B_2 {}^p v = [{}^m \mu_{21}^* {}^m v] \bar{H}_x + [{}^m \mu_{22}^* {}^m v + {}^p \mu_{22} {}^p v] \bar{H}_y.\quad (12b)$$

Here, \bar{D}_x , \bar{D}_y , \bar{B}_x , and \bar{B}_y are the homogenized tangential components of the electric displacement field and magnetic-flux density. Observe that each component of the homogenized magnetic-flux density in Eq. (12b) is related to magnetic fields in both x and y directions. The homogenized tangential components can be expressed as in matrix form as

$$\begin{bmatrix} \bar{D}_x \\ \bar{D}_y \end{bmatrix} = \begin{bmatrix} {}^m \epsilon_{11} {}^m v + {}^p \epsilon_{11} {}^p v & 0 \\ 0 & {}^m \epsilon_{22} {}^m v + {}^p \epsilon_{22} {}^p v \end{bmatrix} \begin{bmatrix} \bar{E}_x \\ \bar{E}_y \end{bmatrix},\quad (13a)$$

TABLE II. Experimental and theoretical magnetoelectric voltage coefficients as obtained by Ref. 17.

| Material | Experimental ME coefficient (maximum) [(V/m)/(kA/m)] | Theoretical ME coefficient [(V/m)/(kA/m)] |
|--|--|---|
| CoFe ₂ O ₄ :PZT-4 | 92.8 | 199–622 |
| CoFe ₂ O ₄ :PZT-8 | 18.6 | 202–634 |
| CoFe ₂ O ₄ :PZT-5H | 74.4 | 143–475 |

$$\begin{bmatrix} B_x \\ B_y \end{bmatrix} = \begin{bmatrix} {}^m \mu_{11}^* {}^m v + {}^p \mu_{11} {}^p v & {}^m \mu_{12}^* {}^m v \\ {}^m \mu_{21}^* {}^m v & {}^m \mu_{22}^* {}^m v + {}^p \mu_{22} {}^p v \end{bmatrix} \begin{bmatrix} H_x \\ H_y \end{bmatrix}.\quad (13b)$$

Observe that the tangential components of the electric field displacement and the magnetic-flux density do not depend on the ME susceptibility tensor. This indicates that the ME effect is only in the direction of the biasing field as should be expected for the longitudinal configuration based upon experimental results.¹⁷

From the second boundary condition, the normal components of the electric displacement and the magnetic-flux density are continuous across the interface. Thus,

$$\begin{aligned}\bar{D}_z &= {}^m D_3 = {}^p D_3, \\ \bar{B}_z &= {}^m B_3 = {}^p B_3.\end{aligned}\quad (14)$$

Here, \bar{D}_z , and \bar{B}_z are the homogenized normal components of the electric displacement field and magnetic-flux density. Applying similar assumption of constant field variation along the thickness of the layer, the homogenized normal components of the electric and magnetic field can be expressed as

$$\begin{aligned}\bar{E}_z &= {}^p E_3 {}^p v + {}^m E_3 {}^m v, \\ \bar{H}_z &= {}^p H_3 {}^p v + {}^m H_3 {}^m v.\end{aligned}\quad (15)$$

Hence, we solve for the homogenized normal component of the electric displacement field and obtain its expression as

$$\bar{D}_z = \frac{(N_1 N_3 - N_5)}{(N_1 N_4 - N_7)} \bar{E}_z + \frac{(N_1 N_2 - N_6)}{(N_1 N_4 - N_7)} \bar{H}_z,\quad (16)$$

where,

$$N_1 = \left[1 + \left(\frac{C_2 {}^p v}{{}^m v {}^p \mu_{33}} \right) \right], \quad N_2 = \left[\frac{{}^p \mu_{33}}{{}^p v} \right], \quad N_3 = \left[\frac{K_2 {}^m v {}^p \mu_{33}}{K_1 ({}^p v)^2} \right],$$

$$N_4 = \left[\frac{{}^m v {}^p \mu_{33}}{K_1 {}^p v} + \left(\frac{K_2 {}^p \mu_{33} ({}^m v)^2}{K_1 {}^m \epsilon_{33} ({}^p v)^2} \right) \right], \quad N_5 = \left(\frac{C_1}{{}^p v} \right), \quad N_6 = \left(\frac{C_2}{{}^m v} \right),$$

TABLE III. Material parameters for magnetostrictive and piezoelectric phases as used in Ref. 17.

| Parameter (units) | CFO | PZT-4 | PZT-8 | PZT-5H | PZT ^a |
|--|-------|-------|-------|--------|------------------|
| s_{11} (10^{-12} m ² /N) | 6.5 | 12.3 | 11.5 | 16.5 | 15.3 |
| s_{12} (10^{-12} m ² /N) | -2.37 | -4.05 | -3.7 | -4.78 | -5 |
| q_{31} (10^{-12} m/A) | 566 | | | | |
| q_{33} (10^{-12} m/A) | 1880 | | | | |
| d_{31} (10^{-12} C/N) | | -123 | -90 | -274 | -175 |
| d_{33} (10^{-12} C/N) | | 289 | 225 | 593 | 400 |
| μ_{33}/μ_0 | 2 | 1 | 1 | 1 | 1 |
| $\varepsilon_{33}/\varepsilon_0$ | 10 | 1300 | 1000 | 3400 | 1750 |

^aReference 21.

$$N_7 = \left(\frac{C_1}{p_V} \frac{m_V}{\varepsilon_{33}} \right). \quad (17)$$

Similarly, the normal component of the magnetic-flux density is obtained as

$$B_z = \frac{(R_1 R_3 - R_5)}{(R_1 R_4 - R_7)} H_z + \frac{(R_1 R_2 - R_6)}{(R_1 R_4 - R_7)} E_z, \quad (18)$$

where,

$$R_1 = \left[1 + \left(\frac{K_2 m_V}{p_V m \varepsilon_{33}} \right) \right], \quad R_2 = \left[\frac{m \varepsilon_{33}}{m_V} \right], \quad R_3 = \left[\frac{C_2 p_V m \varepsilon_{33}}{C_1 (m_V)^2} \right],$$

$$R_4 = \left[\frac{p_V m \varepsilon_{33}}{C_1 m_V} + \left(\frac{C_2 m \varepsilon_{33} (p_V)^2}{C_1 p \mu_{33} (m_V)^2} \right) \right], \quad R_5 = \left(\frac{K_1}{m_V} \right), \quad R_6 = \left(\frac{K_2}{p_V} \right),$$

$$R_7 = \left(\frac{K_1 p_V}{m_V p \mu_{33}} \right). \quad (19)$$

The results obtained show that the constitutive equations for the homogenized ME composite layer has the form

$$\begin{bmatrix} D_x \\ D_y \\ D_z \end{bmatrix} = \begin{bmatrix} 0 & 0 & 0 \\ 0 & 0 & 0 \\ 0 & 0 & \alpha_{zz}^H \end{bmatrix} \begin{bmatrix} H_x \\ H_y \\ H_z \end{bmatrix} + \begin{bmatrix} \varepsilon_{xx} & 0 & 0 \\ 0 & \varepsilon_{yy} & 0 \\ 0 & 0 & \varepsilon_{zz} \end{bmatrix} \begin{bmatrix} E_x \\ E_y \\ E_z \end{bmatrix}, \quad (20a)$$

$$\begin{bmatrix} B_x \\ B_y \\ B_z \end{bmatrix} = \begin{bmatrix} 0 & 0 & 0 \\ 0 & 0 & 0 \\ 0 & 0 & \alpha_{zz}^E \end{bmatrix} \begin{bmatrix} E_x \\ E_y \\ E_z \end{bmatrix} + \begin{bmatrix} \mu_{xx} & \mu_{xy} & 0 \\ \mu_{yx} & \mu_{yy} & 0 \\ 0 & 0 & \mu_{zz} \end{bmatrix} \begin{bmatrix} H_x \\ H_y \\ H_z \end{bmatrix}. \quad (20b)$$

IV. VALIDATION OF THEORETICAL MODEL

The theoretical model is validated via comparison to experimental results obtained by Harshe *et al.*,¹⁷ shown in Table II. We intend to compare our results to measured char-

acteristics of the ME media using the ME voltage coefficient. Through our theoretical model we obtained the ME susceptibility tensor and the effective permittivity, from which we can compute the ME voltage coefficient.

The theoretical model obtained allows for detailed analysis of the ME effect in the composite structure. Analysis can be done on the effects of the interface coupling parameter on the ME media. Increase in volume fraction of either the piezoelectric or magnetostrictive phase can also be analyzed. Based upon such analysis, we can compare our results to other theoretical models and observe the general trends of the ME media. In computing the ME voltage coefficient, we use same material characteristics of the media as given in literature. The material characteristics of the layers are shown in Table III.

We analyze theoretical models for four different ME composites. The first is a composite with CFO for the magnetostrictive phase and PZT-4 for the piezoelectric phase. A plot of the theoretical results for this ME composite is shown in Fig. 2. The ME voltage coefficient increases from zero (piezoelectric volume fraction also equals zero) to a maximum

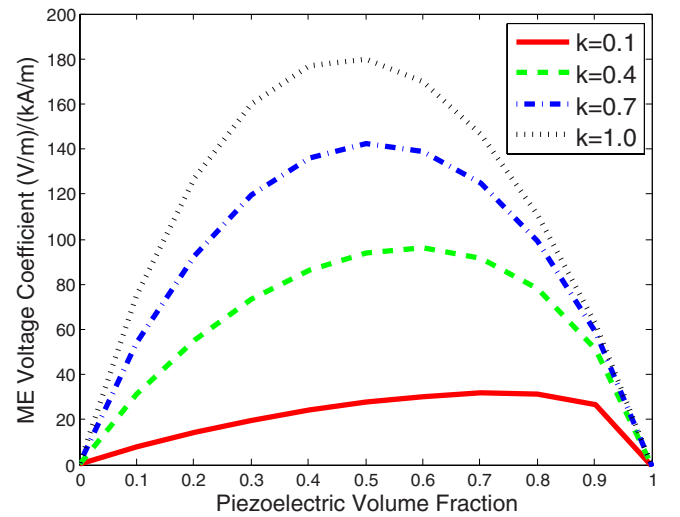


FIG. 2. (Color online) Longitudinal ME coefficient for the ME layer of PZT-4 and CFO. Maximum theoretical ME voltage coefficient obtained is 180 (V/m)/(kA/m). Considering an imperfect interface coupling of 0.4, the value is close to the experimental value of 92.8 (V/m)/(kA/m).

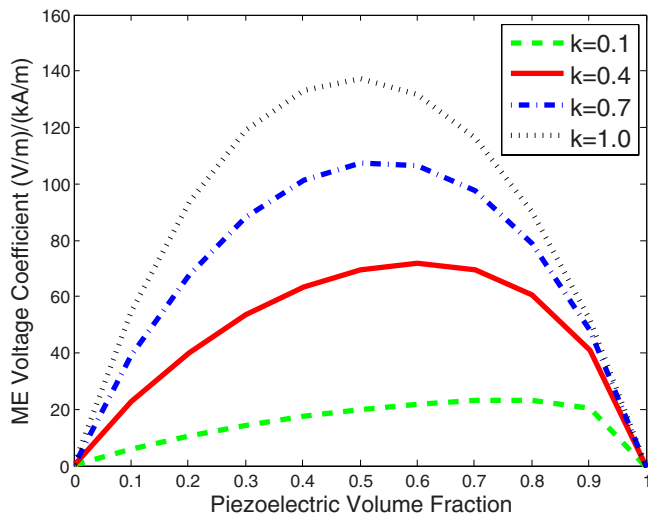


FIG. 3. (Color online) Longitudinal ME coefficient for the ME layer of PZT-5H and CFO. Maximum theoretical ME voltage coefficient obtained is 140 (V/m)/(kA/m). Considering an imperfect interface coupling of 0.4, the value is close to the experimental value of 74.4 (V/m)/(kA/m).

with increasing volume fraction of the piezoelectric phase. This is due to the continuous increase in the elastic interaction between the piezoelectric and magnetostrictive phases. The ME voltage coefficient then decreases to zero as the composite becomes purely piezoelectric (piezoelectric volume fraction equals 1). This result is consistent with the theoretical model obtained by Nan using Green’s-function method.²⁷ From the plots of the ME voltage coefficient for the CFO:PZT-4 composite in Fig. 2, we observe a maximum ME voltage coefficient of 180 (V/m)/(kA/m) obtained for a perfect interface coupling between phases ($k=1$). The maximum experimental value obtained was 92.8 (V/m)/(kA/m). We assume that an imperfect interface and other material factors may be a reason for an approximate 50% loss in the experimental result. Using an interface coupling parameter

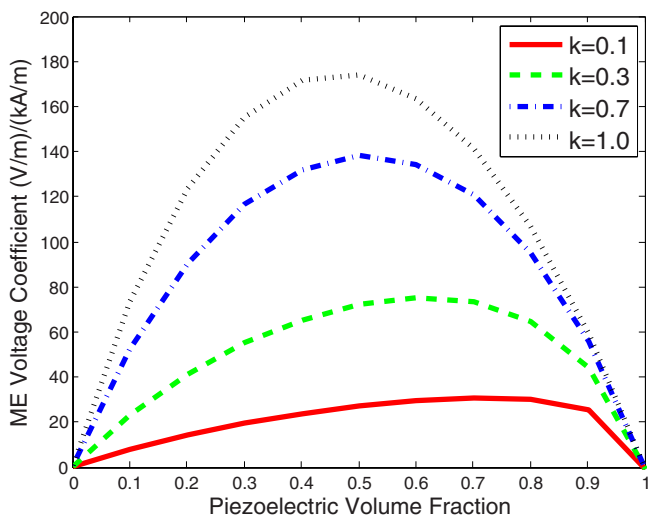


FIG. 4. (Color online) Longitudinal ME coefficient for the ME layer of PZT-8 and CFO. Maximum theoretical ME voltage coefficient obtained is 175 (V/m)/(kA/m).

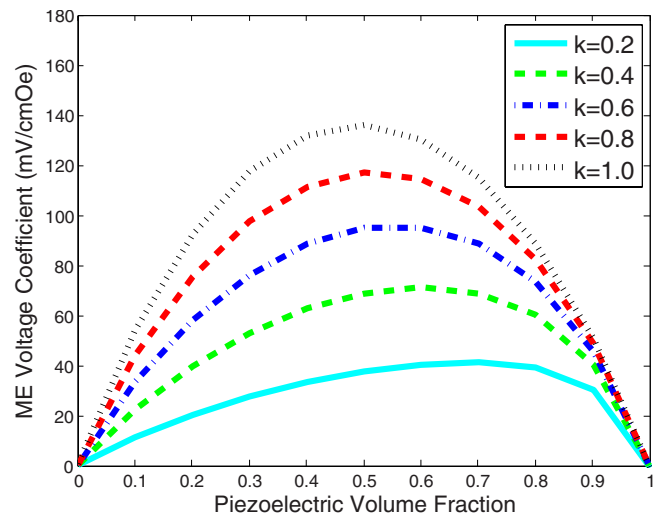


FIG. 5. (Color online) Longitudinal ME coefficient for unclamped CFO-PZT layers as studied in Ref. 21. The plot uses the theoretical model discussed in this paper. The maximum coefficient obtained here (140 mV/cm Oe) is much less than that obtained in Ref. 21 (325 mV/cm Oe).

of 0.4 results in an ME voltage coefficient closer to the experimental data. The results show similar trends to other models as the strength of the ME voltage coefficient decreases as the coupling weakens. Additionally, for weaker coupling, the ME voltage coefficient increases with increase in piezoelectric volume fraction.

Figure 3 shows the theoretical longitudinal ME coefficient for an ME composite consisting of CFO for the magnetostrictive phase and PZT-5H for the piezoelectric phase. Similar trends with the piezoelectric volume fraction are observed for this composition. The maximum theoretical ME voltage coefficient is 140 (V/m)/(kA/m). The experimental value obtained was 74.4 (V/m)/(kA/m). The theoretical results show similar characteristics to available data. We observe that the

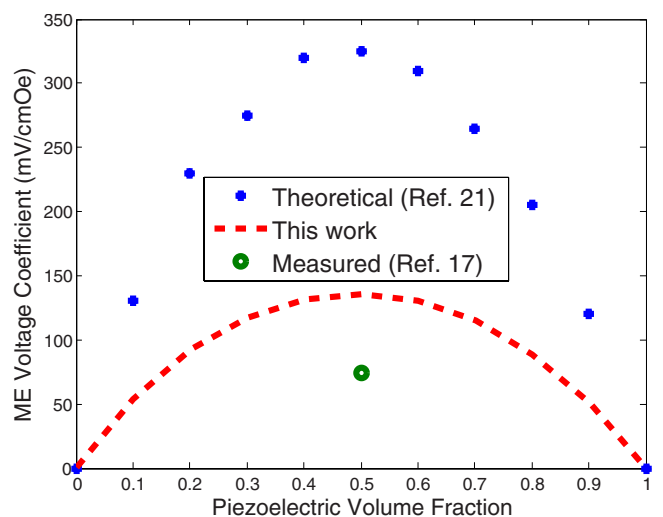


FIG. 6. (Color online) Comparison of the theoretical model for the longitudinal ME voltage coefficient for the unclamped CFO-PZT layer with $k=1$. The theoretical data from Ref. 21 and our work here is compared to experimental data obtained from Ref. 17.

TABLE IV. Comparison of the ME effect obtained for different PZT layers.

| Material type | s_{11} (m ² /N) | s_{12} (m ² /N) | d_{31} (C/N) | ϵ_{33}/ϵ_0 | α' [(V/m)/(kA/m)] |
|---------------|---------------------------------|---------------------------------|-------------------|----------------------------|-----------------------------|
| PZT-4 | 12.3 | -4.05 | -123 | 1300 | 180 |
| PZT-8 | 11.5 | -3.7 | -90 | 1000 | 175 |
| PZT-5 | 16.5 | -4.78 | -274 | 3400 | 140 |

ME voltage coefficient is less than that for PZT-4. This should be expected due to the fact that PZT-5H has a higher relative permittivity than PZT-4. For the CFO:PZT-4 composite, the ME voltage coefficient increases steadily with a maximum value when the phases are equal for the case of a perfect interface coupling. As the interface coupling weakens, the maximum ME coefficient shifts to richer piezoelectric compositions. This trend is consistent with that obtained by Bichurin *et al.*²¹

The plot of the longitudinal ME voltage coefficient for an ME composite with CFO magnetostrictive phase and PZT-8 piezoelectric phase is shown in Fig. 4. The maximum ME voltage coefficient for this composite is 175 (V/m)/(kA/m). The experimental result was obtained as 18.6 (V/m)/(kA/m). The experimental result for this composite is much lower than expected. The reason for such low experimental result is the ineffective method used to bond the layers together.¹⁷ Whereas the more effective tape cast method was used for the CFO:PZT-4 composite, glue was used to bond the CFO:PZT-8 layers, hence resulting in a poor interface coupling between the phases. This composition of CFO:PZT-8 is expected to have comparable ME voltage coefficient to CFO:PZT-4 as their permittivity and piezoelectric coefficients are close in value.

The theoretical models obtained here leads to the observation that for a high longitudinal ME voltage coefficient, the piezoelectric phase should have a high piezoelectric coefficient (d_{31}), and a low permittivity. This is due to the direct relationship between the piezoelectric coefficient and the ME voltage coefficient. The ME voltage coefficient has an inverse relationship with the effective permittivity of the piezoelectric phase, hence the requirement of a piezoelectric phase with low relative permittivity.

Finally, we show results of theoretical model of an unclamped ME composite with CFO for the magnetostrictive phase and PZT for the piezoelectric phase as studied in Ref. 21. The plot of the ME voltage coefficient for our theoretical

model is shown in Fig. 5. We observed similar trends in the behavior of ME voltage coefficient, such as the direct relationship between the interface coupling parameter and the magnitude of the ME voltage coefficient. Also, the maximum ME voltage coefficient shifts to piezoelectric-rich composites for cases with less than perfect coupling. The magnitude of the ME voltage coefficient obtained is less than 140 mV/cm Oe compared to over 300 mV/cm Oe in previous works,²¹ as can be observed in Fig. 6. Hence, we show that the current theoretical model better approximates the ME voltage coefficient in terms of its magnitude while maintaining established trends for the ME material.

V. CONCLUSION

A distinct theoretical model for the longitudinal ME voltage coefficient in a composite made up of magnetostrictive and piezoelectric phases has been obtained. The model better characterizes the ME voltage coefficient of ME bilayers. Using continuity conditions on fields within the composite, we are able to obtain parameters for the ME media. The theoretical model significantly reduces the deviation between the magnitude of theoretical models and experimental data while maintaining the established trends of the ME voltage coefficient. The theoretical model includes expressions for the effective permeability, permittivity, and ME susceptibility tensor of the bilayer. Analysis of the theoretical model shows that lower permittivity materials give a higher ME voltage coefficients due to their inverse relationship. Piezoelectric materials with low compliance coefficients and high piezoelectric coefficients are best fit to create high ME voltage coefficient composites. This can be observed in Table IV.

ACKNOWLEDGMENT

This research project was sponsored by the AFOSR GameChanger Program, Grant No. FA9550-07-1-0462.

¹W. C. Rontgen, *Ann. Phys.* **35**, 264 (1888).

²H. A. Wilson, *Philos. Trans. R. Soc. London, Ser. A* **204**, 121 (1905).

³J. A. Kong, *Electromagnetic Wave Theory*, 2nd ed. (Wiley, New York, 1990), p. 5; *Electromagnetic Wave Theory*, 2nd ed. (Wiley, New York, 1990), pp. 25–28.

⁴L. D. Landau and E. M. Lifshitz, *Electrodynamics of Continuous Media* (Pergamon, Oxford, 1960).

⁵P. Curie, *J. Phys. Theor. Appl.* **3**, 393 (1894).

⁶B. D. H. Tellegen, *Philips Res. Rep.* **3**, 81 (1948).

⁷I. E. Dzyaloshinskii, *Sov. Phys. JETP* **10**, 628 (1959).

⁸D. N. Astrov, *Sov. Phys. JETP* **11**, 708 (1960); **13**, 729 (1961).

⁹V. J. Folen, G. T. Rado, and E. W. Stalder, *Phys. Rev. Lett.* **6**, 607 (1961).

¹⁰G. T. Rado and V. J. Folen, *Phys. Rev. Lett.* **7**, 310 (1961).

¹¹M. Fiebig, *J. Phys. D: Appl. Phys.* **38**, R123 (2005).

- ¹²J. van Suchtelen, Philips Res. Rep. **27**, 28 (1972).
- ¹³J. van den Boomgaard, A. M. J. G. van Run, and J. van Suchtelen, *Ferroelectrics* **10**, 295 (1976); **14**, 727 (1976).
- ¹⁴J. Ryu, A. V. Carazo, K. Uchino, and H. E. Kim, *Jpn. J. Appl. Phys., Suppl.* **40**, 4948 (2001).
- ¹⁵G. Srinivasan, E. T. Rasmussen, J. Gallegos, R. Srinivasan, Y. I. Bokhan, and V. M. Laletin, *Phys. Rev. B* **64**, 214408 (2001).
- ¹⁶J. Ryu, S. Priya, K. Uchino, and H. E. Kim, *J. Electroceram.* **8**, 107 (2002).
- ¹⁷G. Harshe, Ph.D thesis, The Pennsylvania State University, 1991; G. Harshe, J. O. Dougherty, and R. E. Newnham, *Int. J. Appl. Electromagn. Mater.* **4**, 145 (1993).
- ¹⁸C.-M. Chang and G. P. Carman, *J. Intell. Mater. Syst. Struct.* **19**, 11 (2008).
- ¹⁹M. I. Bichurin, V. M. Petrov, and G. Srinivasan, *J. Appl. Phys.* **92**, 7681 (2002).
- ²⁰G. Srinivasan, E. T. Rasmussen, and R. Hayes, *Phys. Rev. B* **67**, 014418 (2003).
- ²¹M. I. Bichurin, V. M. Petrov, and G. Srinivasan, *Phys. Rev. B* **68**, 054402 (2003).
- ²²R. M. Cristensen, *Mechanics of Composite Materials* (Wiley, New York, 1979); D. R. Smith and J. B. Pendry, *J. Opt. Soc. Am. B* **23**, 391 (2006); I. Getman, *Ferroelectrics* **162**, 45 (1994).
- ²³R. E. Newnham, D. P. Skinner, and L. E. Cross, *Mater. Res. Bull.* **13**, 525 (1978).
- ²⁴D. M. Pozar, *Microwave Engineering* (Wiley, New York, 2005).
- ²⁵B. Lax and K. J. Button, *Microwave Ferrites and Ferrimagnetics* (McGraw-Hill, New York, 1962).
- ²⁶R. E. Collin, *Foundations for Microwave Engineering* (McGraw-Hill, New York, 1992).
- ²⁷C.-W. Nan, *Phys. Rev. B* **50**, 6082 (1994).